

A Batteryless Beacon Based on Dual ISM-Band RF Harvesting with Solar-Biasing Current

Wen-Chan Shih[#], Pai H. Chou[†], Wen-Tsuen Chen^{#*}

[#]Institute of Information Science, Academia Sinica, Taiwan

[†]Department of Electrical Engineering and Computer Engineering, University of California, Irvine, USA

^{*}Department of Computer Science, National Tsing Hua University, Taiwan

teddy.shih@iis.sinica.edu.tw, phchou@uci.edu, chenwt@iis.sinica.edu.tw

ABSTRACT

We propose a Bluetooth Low Energy (BLE) beacon that operates entirely on harvested energy from dual ISM-band RF sources with aid from photovoltaics. Indoor RF power can be harvested from Wi-Fi devices in both 2.4 GHz and 5 GHz bands. Indoor photovoltaic power, while often too low to be considered useful, can be used as biasing current to improve the efficiency of the RF harvester. The proposed harvester performs impedance matching in two bands and maximum power point tracking and stores energy in a solid-state battery and a supercapacitor. Our implementation of the energy-neutral BLE beacon can broadcast every 45 seconds at the input power of 15 dBm. In terms of harvested power, our proposed system harvests more power from both bands in a miniature, low-cost circuit than the state-of-the-art from three channels in a single band. This work represents a step towards enabling a class of IoT systems to operate entirely on harvested indoor RF power.

CCS Concepts

•Computer systems organization → Embedded hardware;

Keywords

Wi-Fi; ISM-band; energy harvesting; solar current.

1. INTRODUCTION

Beacon are broadcasting nodes used for indoor localization and navigation, advertising in commercial settings, and exhibits guidance in museums. Beacons can be costly to install if operated by wired power, whereas battery-powered ones may be cheaper to install but costly to replace or recharge batteries. Energy harvesting for beacons can go a long way towards saving significant costs for installation and maintenance.

Ambient power in different forms can be harvested by photovoltaic (PV), thermoelectric, piezoelectric, and RF converters. Outdoor beacons can easily get powered by PV, which has the highest power density among energy harvesting sources. Indoor beacons, in contrast, rely mostly on batteries or wired power. This is because most ambient power available for energy harvesting has been rather

scarce. Other sources include harvesting from ventilation power, but they limit the placement of the beacons or the harvesters.

The other challenges are low voltage and low current from a small solar cell in an environment with low indoor lighting. Existing PV has high energy conversion efficiency in direct sunlight outdoor [10] but not indoor. Indoor PV may output sufficiently high open-circuit voltage, but the current is too low or the internal resistance is too high, such that either the voltage will not overcome the forward voltage of a diode, or it outputs μA -level current, which is by itself too low to be useful for most purposes. As a result, indoor PV power is usually wasted unless the panel is sufficiently large [3], but the size may be too large for beacons. However, we make the observation that it may still be useful for enhancing the output power and efficiency for other types of harvesters.

One new source of indoor power harvesting is Wi-Fi radiation. Wi-Fi is ubiquitous and has been improving in expanding to more bands from 2.4 GHz to 5 GHz. Also, MIMO beamforming, which uses multiple antennas cooperatively to form an RF beam in one direction, improves *directivity* of Wi-Fi power. However, the challenges of multiple ISM-band harvester include impedance matching for multiple frequency bands, low-cost material, and small form factor. Existing Wi-Fi energy harvesters focus on one ISM-band, such as 2.4 GHz [4, 7, 9]. Sub-GHz, non-Wi-Fi RF signals can be harvested, too [15, 16], but it requires an RFID reader, TV towers, or cellular base stations nearby as transmitters. This limits the placement of devices and the accumulated energy, as the conventional impedance matching does not work well for multiple frequency bands.

To capture more of the available RF power, we propose a system that consists of an impedance matching network, a dual-band Wi-Fi energy harvester with a solar cell, a maximum power point tracking (MPPT) subsystem with a solid state battery and a supercapacitor, and a BLE node. We propose a systematic way to design a dual-band impedance matching network using FR4 substrate. The same matching circuit is shown to achieve better return loss and impedance on two frequency bands than the theoretical design on a single frequency band by applying ISM-band diodes and our matching approach. Moreover, as the load affects the return loss and impedance, our system performs MPPT to enhance the power conversion efficiency and load matching. Furthermore, our system employs a supercapacitor as an energy buffer.

We observe that the bias current of an RF Schottky diode increases its output voltage. A novelty with our design is that we exploit the weak PV current under low-luminance condition to reinforce the bias current of RF Schottky diode [1]. This increases the RF-to-DC conversion efficiency, thereby enhancing the output power and efficiency as well. Empirical results confirmed its superior performance to the state-of-the-art [21]. This enables our

Permission to make digital or hard copies of all or part of this work for personal or classroom use is granted without fee provided that copies are not made or distributed for profit or commercial advantage and that copies bear this notice and the full citation on the first page. Copyrights for components of this work owned by others than ACM must be honored. Abstracting with credit is permitted. To copy otherwise, or republish, to post on servers or to redistribute to lists, requires prior specific permission and/or a fee. Request permissions from permissions@acm.org.

ENSsys 2016 November 16, 2016, Stanford, CA, USA

© 2016 ACM. ISBN 978-1-4503-4532-3/16/11...\$15.00

DOI: <http://dx.doi.org/10.1145/2996884.2996886>

implementation of the BLE beacon to advertise once every 45 seconds, and it represents a step towards making RF harvesting practical for an important class of IoT applications. The contributions of our design are threefold. First, we adopt the solar bias current to improve efficiency of Wi-Fi energy harvesting. Second, we propose a dual ISM-band energy harvester to increase harvested power. Third, we show the applicability of the proposed energy harvester to operating a BLE beacon in an energy-neutral way.

2. RELATED WORK

Energy harvesting devices and platforms have been proposed to improve the operating lifetime of deeply embedded systems in a wide range of IoT applications. This section reviews existing energy harvesting technologies from RF, indoor PV and thermoelectric sources.

2.1 RF Energy Harvesting

The output power of energy harvesters from ambient RF sources is usually too low to sustain today’s microcontroller units (MCU) [9]. As a result, RF energy harvesting has been limited to specialized systems either by backscattering or band-specific impedance matching. Backscattering transforms the RF source signals into another reflected signal that encodes the information to be retrieved. For example, Sample et al [19] is a backscattering system that operates on RF power emitted by a 1 MW TV tower in direct line-of-sight. Up to $60 \mu\text{W}$ that can be converted, although it must be located close to the TV tower [23]. Its use as a more general power supply for embedded systems still remains to be seen.

RF power in different frequency bands can be harvested, but each requires a separate impedance matching circuit [8, 15, 16]. Niotaki et al [13] proposes a dual-band rectenna operating at 915 MHz and 2.45 GHz. The rectenna consists of an antenna and an impedance matching circuit and a RF diode to convert RF signal to DC power. While this is close to our a single impedance matching circuit for two frequency bands, we design the impedance matching circuit for two higher frequency bands of 2.4 GHz and 5 GHz of dual Wi-Fi frequency bands and the bias current for further improving the RF-DC conversion efficiency. The design of higher frequency bands has more challenges. First, the component of circuit is more sensitivity with parasitic capacitance and stray inductance. Second, it requires a fine-tuning on various FR4 PCBs for evaluation.

Using wireless beamforming methods to provide an alternative power source is discussed in existing works. There is still a problem regarding improvement of RF-to-DC conversion. Techniques that use conventional Wi-Fi APs at home or public areas as the RF energy transmitter have been proposed [4, 7]. These works motivate us to harvest Wi-Fi power and increase the RF-to-DC conversion efficiency for most wearable devices. Some study has been proposed to optimize beamforming vectors and power configurations [22] for existing harvesters. However, we design a system using a dual-ISM-band harvester and a solar bias current to collect more power than existing single-band and dual-band harvesters. The beamforming of IEEE 802.11ac-compliant APs represents a promising technology that can bring the order of magnitude improvement needed to make it viable, but it still needs to be explored further [20].

2.2 Indoor Photovoltaics

The PV energy harvesting technologies are improved by a MPPT approach and Schottky diodes in the literature. Scavenging a weak solar power still remains to be a challenge. Indoor PV requires either two large solar panels [3] or a small solar cell with the high PV conversion efficiency under weak indoor light condition. We

observe that a bias current of a RF Schottky diode increases its output voltage [1]. The maximum output voltage is 38 mV at the bias current of $5 \mu\text{A}$ under the input power of -30 dBm at frequency of 2.45 GHz with load resistance of $100 \text{ k}\Omega$. A bias current between 0.4 and $20 \mu\text{A}$ is required to keep the maximum output voltage above 50%. In the theoretical analysis, a PV surface area of $6 \text{ mm} \times 6 \text{ mm}$ is required to achieve $10 \mu\text{W}$ (i.e., $14.97 \mu\text{A} \times 0.7 \text{ V}$ under the indoor low light density of $100 \mu\text{W}/\text{cm}^2$ and the indium gallium phosphide (InGaP) PV conversion efficiency of 29.1% [11, 18]. Besides RF, Bandyopadhyay et al [2] proposes parallel converters for multiple energy sources to improve the efficiency, such as PV, thermoelectric, and piezoelectric. The system performs MPPT, but it works primarily on PV sources and does not include RF energy harvesting.

Gummeson et al [5] utilizes a miniature solar panel as the other DC power source and ambient light energy to increase the Intel WISP sensor range and data rate. Although this work is close to our idea and our design can function as a DC power source as well, there are three main differences from our design. First, we focus on a bounded range of solar bias current (between 0.8 to $9 \mu\text{A}$ to sustain $\geq 80\%$ maximum output voltage at the input power of -30 dBm and 2.45 GHz) to increase the RF diode’s RF-to-DC conversion efficiency. Second, based on our design, we suggest that a semiconductor design house can consider including a miniature solar cell inside a RF diode to enhance the RF diode’s output voltage and detection sensitivity. Thirdly, we concentrate on popular Wi-Fi AP’s power with the dual frequency bands rather than an RFID reader’s power with a single UHF band in the indoor environment.

2.3 Thermoelectric Energy Harvesting

Thermoelectric harvesting requires another small energy source to assist with the startup voltage. This is a similar idea as our design using an extra solar biasing current to increase the RF-to-DC efficiency. Thermoelectric energy harvesting requires a startup voltage, which may be generated by a battery or a secondary harvesting source such as human vibration power or RF power. Ramadass et al [17] proposes a batteryless thermoelectric energy harvesting circuit to collect thermal energy from human body heat. One notable feature is that it requires a startup voltage of 35 mV to enable operation of the circuit, which is obtained by a separate motion-harvesting circuit from human vibration. A similar study has been proposed in an ultra low-power batteryless energy harvesting body sensor node for electrocardiogram (ECG), electromyogram (EMG), and electroencephalogram (EEG) applications. Zhang et al [24] presents a thermal harvesting circuit that requires the startup voltage of 600 mV. They propose an RF-harvesting circuit from a 433 MHz transmitter to provide a startup voltage at the RF pulse power of -10 dBm for two seconds. Those thermoelectric energy harvesting circuits adopt vibration and RF pulse power to enable the startup circuit.

3. SYSTEM DESIGN

This section describes our system design. We first present a system overview, followed by a description for each component. We tune our design for the maximum power conversion efficiency (PCE) and select proper components for impedance matching.

3.1 System Overview

Fig. 1 shows our harvester prototype. The system is composed of the impedance matching network, the one-stage charge pump circuit, the MPPT module with energy storage unit, and the BLE node. The energy of wireless AC voltage source V_s is delivered to capacitor C_{out} through the matching network in terms of L_m, C_m ,

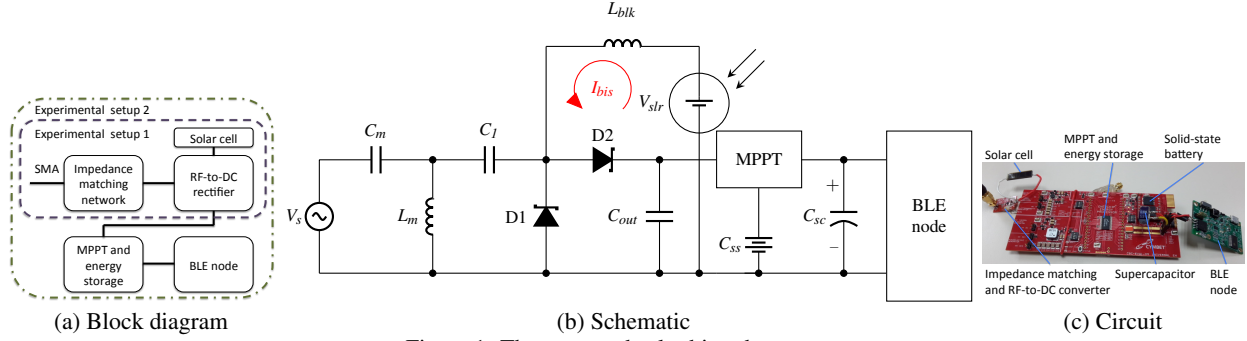


Figure 1: The proposed solar biased prototype

and diodes D_1 and D_2 . The MPPT module supports impedance adjustment to achieve maximum power delivery. C_{ss} and C_{sc} work as energy buffers. Finally, the accumulated energy powers the BLE node.

3.2 Impedance-Matching Network

We select the proper capacitor C_m and the inductor L_m for the impedance matching network. We experiment with the component one by one for impedance matching. In the impedance matching process, L_m and C_m are adjusted to match the two frequency bands of 2.4 GHz and 5 GHz through the return loss and impedance measurement. The important factors affect the impedance, such as traces and a thickness of circuit. Therefore, if the values of L_m and C_m are difficult to obtain, we refine the traces and the thickness of circuit for achieving the impedance of 50Ω through resizing the circuit board and redesign. Moreover, cutting the edge of the circuit board can improve the impedance matching as it reduces effects from parasitic capacitances. The main idea is to achieve the maximum PCE through load and frequency adjustments. There are three main steps to finish load and frequency adjustments to obtain the global maximum PCE. First, we adjust the load resistor to accomplish the local maximum PCE at the fixed frequency. Second, we change frequencies in a single frequency band to complete the local maximum PCE. Finally, we find the proper load and frequency settings to operate at the global maximum PCE in two frequency bands. Solving for the PCE yields

$$\text{PCE} = \frac{P_{out}}{P_{in}}, \quad (1)$$

where $P_{out} = \frac{V_{out}^2}{R}$.

3.3 RF-to-DC Rectifier

Fig. 1c shows our circuit that consists of Greinacher voltage doubler [12] and a small solar cell. The voltage doubler includes capacitors and the microwave Schottky detector diode used as the RF-to-DC power converter [1]. We take advantage of the dual ISM-band feature of our prototype to harvest more energy. Our design can be manufactured by common FR4 substrate that reduces much cost.

3.4 Solar Biased Current

The proposed solar biased design consists of a block inductor (L_{blk}) and a small lightweight solar cell. The block inductor is used to block the RF signal power feeding the solar cell. The small solar cell supports a bias current in low light environment through the block inductor L_{blk} and the microwave Schottky detector diode D_2 . The bias current increases the RF-to-DC conversion efficiency of

D_2 to enhance the output power P_{out} and PCE of our prototype [1]. We take advantage of the bias current from a small solar cell under a low illuminance condition to increase the detection sensitivity of the microwave Schottky detector diode.

For proof of concept, we choose a small lightweight solar cell, the IXYS KXOB22-01X8 with open-circuit voltage of 4.7 V and short-current current of 4.4 mA at one sun ($100\text{ mW}/\text{cm}^2$) condition, size of $22 \times 7 \times 1.8\text{ mm}$ [6], and the weight of 0.5 g. We use $L_{blk} = 1\text{ nH}$ as the block inductor. The bias current is from the dark indoor environment with about 200 lux of ambient light.

3.5 MPPT and Energy Storage

We place an additional supercapacitor of 0.1 F with the rated voltage of 5.5 V on the output of the MPPT module. The supercapacitor has been charged before experiment to speed up powering the BLE node. To maximize power transfer, we use the MPPT module to change operation point by its automatic load adjustment. The MPPT module uses an energy storage as a load.

The energy storage includes the solid state battery, C_{ss} , and the supercapacitor, C_{sc} . As our prototype takes advantage of the MPPT module in the Cymbet evaluation board with the built-in $100\text{ }\mu\text{Ah}$ solid-state battery module and an extra supercapacitor of 0.1 F with the rated voltage of 5.5 V. The supercapacitor of 0.1 F is manufactured by Panasonic [14], called ‘‘Gold Capacitor.’’ As we charge the supercapacitor before our experiment, our system can support the built-in BLE node doing the fast burst advertising.

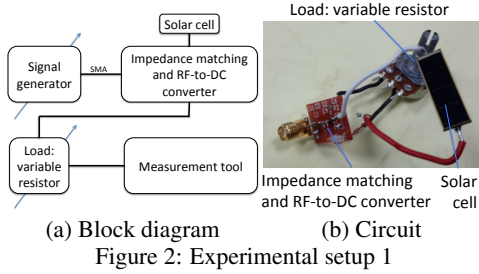
For accumulating more energy to sustain the high peak transmit power of the BLE node, the additional supercapacitor C_{sc} has been added on the output of the MPPT module.

3.6 BLE Node

The BLE node is used to work as a BLE beacon. Its transmit power is 0 dBm for advertising packets. To implement the low power operation, we duty-cycle active mode for one second and low-power sleep mode (PM2) for 45 seconds. A sleep timer in PM2 is used to wake up BLE node from sleep mode.

4. EXPERIMENTAL EVALUATION

To evaluate our harvester’s performance, we build a prototype of our proposed batteryless beacon to operate on harvested Wi-Fi power from both 2.4 GHz and 5 GHz bands with aid from indoor PV for biasing. In this section, we describe the experimental setups and observations from empirical results. We have two experimental setups. The first is the same as the state-of-the-art [21] for evaluating the harvester without the BLE node for fairness of comparison. The second setup includes the MPPT module and supercapacitor to power a BLE node.



4.1 Setup 1: Harvester Only

The experiment scenario is to change transmit power, transmit frequency, and load to explore the enhancement of our proposed design concept. Fig. 2 shows our first experimental setup, including a signal generator, our wireless energy harvesting prototype, load, and a multimeter. Currently, a multimeter is used for voltage measurement as a start point. We will apply the other MCU and its ADC to obtain higher precision measurements in the future work. The BLE node is excluded to focus on evaluating the RF harvester (“front end”). We employ a Rohde & Schwarz SMIQ06B signal generator with a frequency range of 300 kHz to 6.4 GHz as our 2.4 GHz and 5 GHz wireless energy sources. It supports configurations of the frequency and transmit power, P_{in} , that will affect salient characteristics, such as output DC voltage V_{out} , RF-to-DC PCE, and output power P_{out} . We connect the signal generator to our prototype directly through the SMA connector as the concentrated input power on the RF connector can imitate the Wi-Fi beamforming of IEEE 802.11ac. This setup enables us to precisely control the signal strength and frequency to quantify the efficiency of our proposed RF-to-DC conversion circuit with reproducible results. The load comprises variable resistors as we explore its impact on system characteristics. We use the multimeter to measure the V_{out} of the load and then apply Eqn. (1) to compute the RF-to-DC PCE.

4.1.1 Empirical Results

For the maximum wireless power delivery, we investigate impacts of frequency, the input power level, and the load on the output power level.

4.1.2 Frequency and Load Impacts

Fig. 3a, 3b, and 3c show the output voltage, the RF-to-DC PCE, and the output power, respectively, as functions of frequency at P_{tx} of 0 dBm. We sweep the frequencies from 5.045 GHz to 5.745 GHz in a step of 0.1 GHz and set to 2.445 GHz. We observe that the frequency of 5.045 GHz with load of 800 Ω outperforms all other configurations in the RF-to-DC PCE and the P_{out} , though the frequency of 5.245 GHz with load of 10 k Ω achieves the maximum V_{out} . Therefore, we choose the the frequency of 5.045 GHz and 800 Ω as our prefer configurations.

4.1.3 Input Power Impact

To further increase the power transfer, we investigate the impact of P_{in} on P_{out} . Fig. 4a and Fig. 4b show that measured output power increases by about two times when the input power increases by 5 dBm for dual-band of 2.4 GHz and 5 GHz. As a result, we can employ a high-gain antenna or directional antenna with more than 5 dB gain to increase the input power.

4.1.4 Dual ISM-Band Benefit

For increasing the output power of our design, we investigate the dual-ISM-band power at 2 GHz and 5 GHz. To expose the dual-

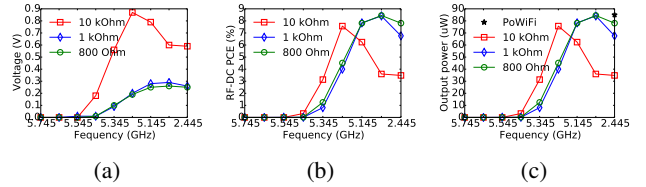


Figure 3: Empirical results as a function of frequency. (a) Output voltage (V_{out}); (b) RF-to-DC power conversion efficiency; (c) Output power (P_{out})

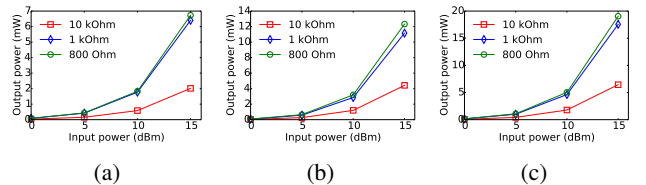


Figure 4: Output power (P_{out}) of our prototype. (a) Frequency at 5.045 GHz; (b) Frequency at 2.445 GHz; (c) Calculation of 2.445 GHz and 5.045 GHz

band benefit, we calculate P_{out} of both frequencies of 2.445 GHz and 5.045 GHz, shown in Fig. 4c. We observe that the P_{out} at 2.445 GHz is higher than the P_{out} at 5.045 GHz.

For output power comparison with existing Wi-Fi harvester, called PoWiFi [21], our design supports crucial features including dual ISM bands (2.4 GHz and 5 GHz). Fig. 3c shows that although our system does not harvest more power than PoWiFi at any signal band of 2.4 GHz or 5 GHz, it takes advantage of dual-ISM-band diode [15] to collect more power than the existing work.

In addition, it achieves the P_{out} of 84.5 μ W and 78.1 μ W at the P_{in} of 0 dBm for 5 GHz and 2 GHz Wi-Fi bands, respectively, while PoWiFi only delivers the P_{out} about 85 μ W across all three Wi-Fi channels at channel 1, 6, and 11 of 2.4 GHz band, shown in Fig. 3c. Consequently, our harvester takes advantage of dual-ISM-band power to collect more power transfer than the existing work.

4.1.5 Solar-Biased Current Enhancement

Fig. 5, 6, and 7 show that our design increases the output power by 6 mW and efficiency by 20% at the frequency band of 5 GHz. But our design only provides small improvements at the frequency of 2.445 GHz.

4.2 Setup 2: Powering BLE node

The second setup reflects conditions to be expected in real-world settings. On the power source side, we set the RF signal generator transmits power at +15 dBm. We also experiment with an Apple Airport Extreme base station with MIMO beamforming set to its maximum power level. On the receiving end, a number of high-gain antennas and patch antennas are tested.

Initial results from Setup 2 are less controllable and less reproducible. The receive power from the initial test is -1 dBm, which is lower than our system’s minimum requirement of input power of 0 dBm. The losses range from -16 to -18 dBm over the air. Therefore, additional work on antenna selection or matching is needed to increase the receive power by 1-3 dBm before the harvester can function. Therefore, we use the signal generator to provide RF power to our system.

4.2.1 Batteryless BLE Landmark

To power our system for the IoT application, such as the battery-

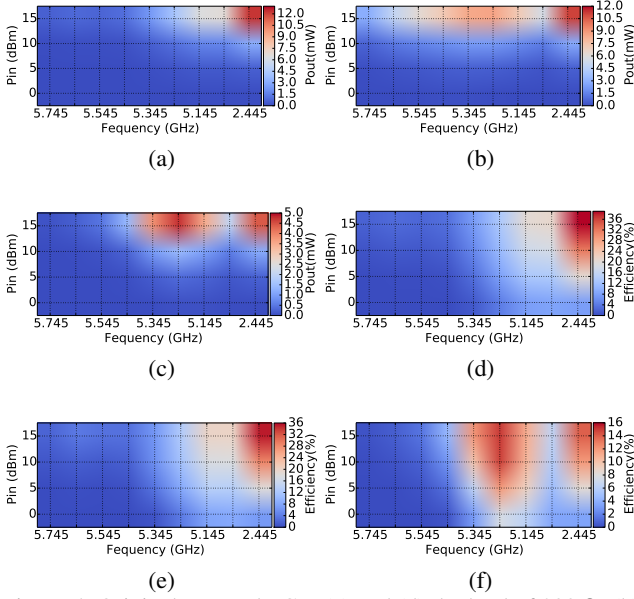


Figure 5: Original P_{out} and PCE. (a) and (d) the load of 800 Ω ; (b) and (e) the load of 1 k Ω ; (c) and (f) the load of 10 k Ω

less landmark in indoor localization, we build the prototype shown in Fig. 8. Fig. 8 shows that the accumulated output voltage of our design is larger than the minimum operation voltage requirement of 2.0 V of the BLE device. The output voltage of the MPPT module of our design should reach 2.61 V to power the BLE device. It will drop to 1.74 V after the BLE device advertising for about one second.

From experiment results, the MPPT module of our design powers the BLE landmark with the fast burst advertising every 45 seconds at P_{in} of 15 dBm, shown in Fig. 8. Therefore, our system can work as a BLE Beacon advertising periodically for indoor localization. It is envisaged that our system is practical and towards batteryless operation for the IoT applications.

We describe problems encountered during experiments and possible methods to overcome. We encounter problems of harvesting antenna selection and have some possible ideas for future work. Currently our prototype works only on RF signal generator's carrier waveform to simulate the Wi-Fi power. Using a high-gain omnidirectional antenna still does not work with a Wi-Fi AP that have tested. The problem is too much power loss of >16 dBm between the Wi-Fi AP's internal antenna and the receiving high-gain omnidirectional antenna. Thus, we only focus on the RF-to-DC conversion efficiency of the harvester circuit rather than antenna selection for harvesting. We have tested that the RF signal generator with the high-gain omnidirectional antenna and a transmit power of +15 dBm losses about 16 dBm over the air as a mismatch between transmitting and receiving omnidirectional antennas and a high-frequency path loss according to the Friis transmission equation. As a result, our system with the high-gain omnidirectional antenna barely receives the input power of -1 dBm (measured by a spectrum analyzer). The low input power is less than our system's minimum requirement of input power of 0 dBm. Thus, it is difficult to harvest any power less than 0 dBm for our system. The possible ideas for solving this problem are using high-gain patch antenna and reduce minimum requirement of input power. Those problems will be the future work.

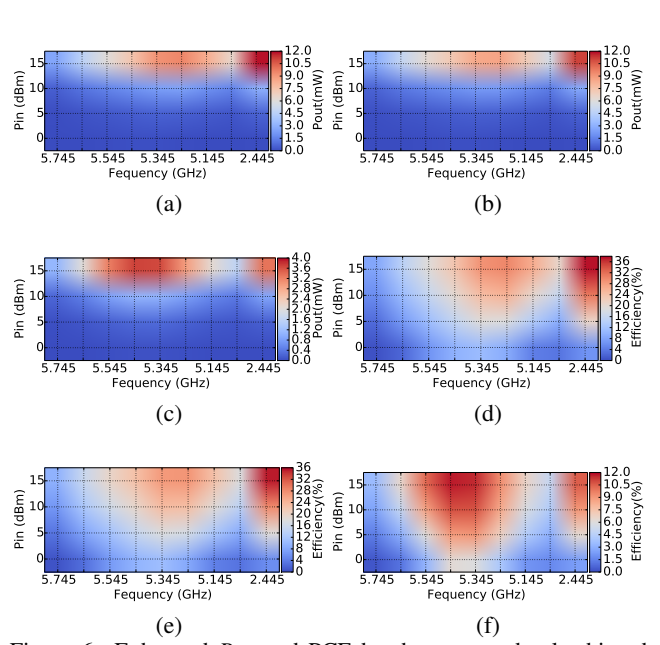


Figure 6: Enhanced P_{out} and PCE by the proposed solar biased current. (a) and (d) the load of 800 Ω ; (b) and (e) the load of 1 k Ω ; (c) and (f) the load of 10 k Ω

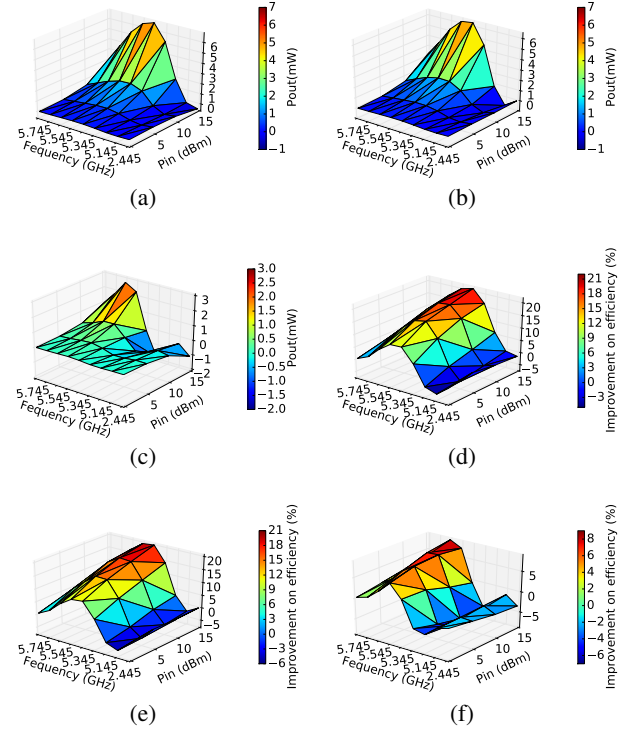


Figure 7: Improvements on P_{out} and PCE by the proposed solar biased current. (a) and (d) the load of 800 Ω ; (b) and (e) the load of 1 k Ω ; (c) and (f) the load of 10 k Ω

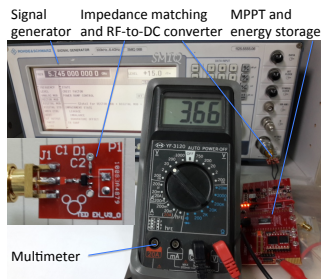


Figure 8: Experimental setup 2: our prototype achieves powering the BLE device advertising for one second in the time period of 45 seconds at P_{in} of 15 dBm

5. CONCLUSION

We propose a batteryless indoor beacon powered by harvested dual ISM-band RF signals and assisted by PV current. We expect the power source to be Wi-Fi signals in both 2.4 GHz and 5 GHz. Indoor PV power can be useful to enhance the RF energy harvesting efficiency. Only our circuit part is validated in setup 1. The validation in a practical setup 2 is still work in progress. We validated the entire batteryless beacon running on harvested power from a signal generator. At this point, the loss over the air is high, even for high-gain antennas. Designing a suitable antenna is a key challenge left to future work. We believe our work represents a promising way towards making RF energy harvesting from Wi-Fi a viable option for the IoT applications.

6. ACKNOWLEDGMENTS

The authors thank Prof. Jen-Ming Wu's communication SOC Lab, National Tsing Hua University, Hsinchu, Taiwan, for instruments support. This research is funded in part by the Thematic Research Program of Academia Sinica under Grant Number 23-24.

7. REFERENCES

- [1] Avago. HSMS-286x surface mount microwave Schottky detector diodes, 2009.
- [2] S. Bandyopadhyay and A. Chandrakasan. Platform architecture for solar, thermal, and vibration energy combining with MPPT and single inductor. *IEEE Journal of Solid-State Circuits*, 47(9):2199–2215, 2012.
- [3] Diversified Power International, LLC. TwinStar, dual 12V 1.5A, dual-channel Delphi connector input and output, 2013.
- [4] S. Gollakota, M. Reynolds, J. Smith, and D. Wetherall. The emergence of RF-powered computing. *Computer*, 47(1):32–39, Jan 2014.
- [5] J. Gummesson, S. S. Clark, K. Fu, and D. Ganesan. On the limits of effective hybrid micro-energy harvesting on mobile CRFID sensors. In *Proceedings of the 8th International Conference on Mobile Systems, Applications, and Services (MobiSys)*, pages 195–208, New York, NY, USA, 2010.
- [6] IXYS. IXOLAR SolarBIT: KXOB22-01X8, 2011.
- [7] B. Kellogg, A. Parks, S. Gollakota, J. R. Smith, and D. Wetherall. Wi-Fi Backscatter: Internet connectivity for RF-powered devices. In *Proceedings of ACM SIGCOMM*, August 2014.
- [8] S. Keyrouz, H. Visser, and A. Tjhuis. Multi-band simultaneous radio frequency energy harvesting. In *Proceedings of the 7th European Conference on Antennas and Propagation (EuCAP)*, pages 3058–3061, April 2013.
- [9] V. Liu, A. Parks, V. Talla, S. Gollakota, D. Wetherall, and J. R. Smith. Ambient backscatter: wireless communication out of thin air. In *Proceedings of the ACM SIGCOMM*, pages 39–50, New York, NY, USA, 2013.
- [10] I. Mathews, G. Kelly, P. J. King, and R. Frizzell. GaAs solar cells for indoor light harvesting. In *2014 IEEE 40th Photovoltaic Specialist Conference (PVSC)*, pages 0510–0513, June 2014.
- [11] B. Minnaert and P. Veelaert. A proposal for typical artificial light sources for the characterization of indoor photovoltaic applications. *Energies*, 7(3):1500, 2014.
- [12] A. Nimo, D. Grgić, and L. M. Reindl. Optimization of passive low power wireless electromagnetic energy harvesters. *Sensors*, 12(10):13636, 2012.
- [13] K. Niotaki, S. Kim, S. Jeong, A. Collado, A. Georgiadis, and M. Tentzeris. A compact dual-band rectenna using slot-loaded dual band folded dipole antenna. *Antennas and Wireless Propagation Letters, IEEE*, 12:1634–1637, 2013.
- [14] Panasonic. EECF5R5H104, 0.1 F, 5.5 V, electric double layer capacitors (Gold Capacitor), 2016.
- [15] A. Parks and J. Smith. Sifting through the airwaves: Efficient and scalable multiband RF harvesting. In *Proceedings of the 2014 IEEE International Conference on RFID (IEEE RFID)*, pages 74–81, April 2014.
- [16] A. Parks and J. Smith. Active power summation for efficient multiband RF energy harvesting. In *Microwave Symposium (IMS), IEEE MTT-S International*, pages 1–4, May 2015.
- [17] Y. Ramadass and A. Chandrakasan. A battery-less thermoelectric energy harvesting interface circuit with 35 mV startup voltage. *IEEE Journal of Solid-State Circuits*, 46(1):333–341, 2011.
- [18] J. A. Russo, W. Ray, M. S. Litz, and C. Wu. Low illumination light (LIL) solar cells: Indoor and monochromatic light harvesting, November 2015.
- [19] A. Sample and J. Smith. Experimental results with two wireless power transfer systems. In *Proceedings of IEEE Radio and Wireless Symposium (RWS)*, pages 16–18, 2009.
- [20] W.-C. Shih, P. H. Chou, and W.-T. Chen. Empirical validation of Energy-Neutral operation on wearable devices by MISO beamforming of IEEE 802.11ac. In *Proceedings of the 2nd International Workshop on Energy Neutral Sensing Systems (ENSSys)*, November 2014.
- [21] V. Talla, B. Kellogg, B. Ransford, S. Naderiparizi, S. Gollakota, and J. R. Smith. Powering the next billion devices with Wi-Fi. *CoRR*, abs/1505.06815, 2015.
- [22] S. Timotheou, I. Krikidis, G. Zheng, and B. Ottersten. Beamforming for MISO interference channels with QoS and RF energy transfer. *IEEE Transactions on Wireless Communications*, 13(5):2646–2658, May 2014.
- [23] Y.-H. Tu, Y.-C. Lee, Y.-W. Tsai, P. H. Chou, and T.-C. Chien. EcoCast: Interactive, object-oriented macroprogramming for networks of ultra-compact wireless sensor nodes. In *Proceedings of the 10th International Conference on Information Processing in Sensor Networks (IPSN)*, 2011.
- [24] Y. Zhang, F. Zhang, Y. Shakhsheer, J. Silver, A. Klinefelter, M. Nagaraju, J. Boley, J. Pandey, A. Shrivastava, E. Carlson, A. Wood, B. Calhoun, and B. Otis. A batteryless 19 μ W MICS / ISM-band energy harvesting body sensor node SoC for ExG applications. *IEEE Journal of Solid-State Circuits*, 48(1):199–213, Jan 2013.